Chemical and Structural Properties of the Inclusion Complex of Euplotin C with Heptakis(2,6-di-*O*-methyl)-β-cyclodextrin through NMR Spectroscopy, Electrospray Mass Spectrometry and Molecular Mechanics Investigations

Graziano Guella,*[a] Emanuela Callone,[a] Ines Mancini,[a] Gloria Uccello-Barretta,[b] Federica Balzano,[b] and Fernando Dini[c]

Keywords: Euplotin C / Cyclodextrins / NMR spectroscopy / Electrospray ionization / Hydrolysis

The inclusion complex of heptakis(2,6-di-*O*-methyl)-β-cyclodextrin (DIMEB) with euplotin C (EC), a cytotoxic metabolite isolated from the protistan strains composing the marine ciliate *Euplotes crassus,* has been investigated by ^{1}H NMR techniques, electrospray ionization mass spectrometry (ESI/MS) and molecular mechanics (MM) calculations. The results suggest that DIMEB preferentially includes the side chain of this sesquiterpenoid with the terminal methyl groups exposed at the narrower rim of the cyclodextrin (CD). The dihydropyranic ring of EC is also well enclosed in the host cavity, whereas the acetyl group and the ring protons at C-4 and C-5 lie outside the larger rim. A kinetic degradation study of EC and its inclusion complex (EC-DIMEB) in aqueous solution has been performed by HPLC-UV-MS measurements obtaining structural data for the hydrolysis end-products. A significant increase in the chemical stability of complexed EC compared with free EC has also been determined.

Introduction

Euplotin C (EC) (**1**, Scheme 1) is the principal one of four secondary metabolites isolated [1] from strain cultures of the cosmopolitan morphospecies *Euplotes crassus* (Dujardin, 1841), representing a reliable chemotaxonomic marker of this species described on the basis of the outward appearance. In fact, whatever the geographical origin and the culturing conditions, strains of *E. crassus* have been found to produce EC as the major metabolite. Although chemotaxonomy has been widely exploited by natural products chemists at genus, family or higher taxonomic levels, the ability of EC to identify *E. crassus* among other species of the same genus gives it a taxonomic significance at the species level. Moreover, EC has been found to be strongly cytotoxic against other non-producer ciliates, even those belonging to closely related morphospecies, such as *E. vannus* and *E. minuta*, [2] and a lethal dose as low as 0.5 μg/mL is able to kill 100% of TB6 (*E. vannus*) cells. More recently, we have found that EC provides a dose-dependent effect on other harmful eukaryotic microorganisms, the flagellates *Leishmania major* and *L. infantum*, responsible for the cutaneous and visceral leishmaniasi diseases, respectively.[3]

The chemical features of this sesquiterpene, whose structure has been elucidated at the absolute configuration level,[1c] are: i) the new tricyclic skeleton, ii) the trialdehyde-masked system contained within the tricyclic ring system and iii) the 2,6 *trans* stereochemistry at the cyclopentane ring which gives to EC and to its closely related analogues euplotin A (**2**, Scheme 1) and euplotin B a much higher degree of strain than the diastereomeric 2,6 *cis* analogue udoteatrial hydrate,[4] a diterpenoid isolated from the marine algae *Udotea flabellum*. According to our PM3 semi-empirical calculations, the difference of strain energy between EC and its C-6 epimer is expected to be as high as 12 kcal/mol, a structural feature somehow per se sufficient to explain the high chemical instability of all the euplotins. It is also worthy of mention that euplotin A (**2**, Scheme 1) in racemic form has recently been synthesized,[5] even if the overall yield of this synthetic procedure is quite low.

Peculiar physicochemical characteristics for EC derive from the chemical/structural features stressed above. First of all, EC is unstable even in a mild basic hydrolytic medium; in fact, once the acetyl function at C-15 of euplotin

[a] Laboratorio di Chimica Bioorganica, Dipartimento di Fisica, Università di Trento,
via Sommarive 14, 38050 Povo-Trento, Italy
Fax: (internat.) +39-0461-882009
E-mail: guella@science.unitn.it
[b] Dipartimento di Chimica e Chimica Industriale, Università di Pisa,
via Risorgimento 35, 56126 Pisa, Italy
Fax: (internat.) +39-050-918260
E-mail: gub@dcci.unipi.it
[c] Dipartimento di Etologia, Ecologia ed Evoluzione, Università di Pisa,
via Volta 6, 56126 Pisa, Italy
Fax: (internat.) +39-050-24252
E-mail: f.dini@deee.unipi.it

  DOI: 10.1002/ejoc.200300502

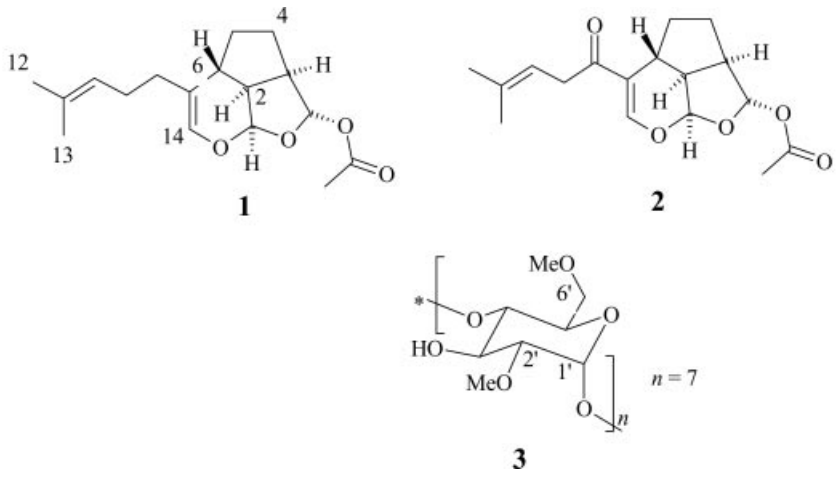

Scheme 1. Chemical structures of euplotin C (**1**), euplotin A (**2**) and heptakis-(2,6-di-*O*-methyl)-β-cyclodextrin (**3**)

C is hydrolyzed, a cascade of irreversible transformations occurs in a very short reaction time.[1c] As described in the last part of this paper, EC can be hydrolyzed even in neutral aqueous media (water or even buffered aqueous solution) when the solution is properly sonicated, even though in such conditions the reaction does not afford the same end-products as those previously observed.[1c] Finally, since EC is a rather hydrophobic compound, its low water solubility represents a serious limitation of the reliability of the biotesting methods. In order to reveal insights into the mechanistic details of the hydrolysis and to overcome these difficulties, we have prepared inclusion complexes of EC with some cyclodextrin (CD) derivatives.

Cyclodextrins are cyclic oligosaccharides, whose three-dimensional structure is similar to a truncated cone, with the ability to accommodate partially/entirely, inside their hydrophobic cavity, a wide variety of guest molecules, forming inclusion complexes with enhanced solubility and improved chemical and physical stability.[6−8] Many chemical aspects of CD have been extensively studied in recent years; in particular, in this context, we were mainly interested in all the aspects relying on improving the guest's characteristics of pharmaceutical interest.[9,10]

The CD class includes three native structures and a broad group of derivatives, which show many different physicochemical characteristics.[11−13] After some complexation trials carried out with different CD derivatives using NMR techniques and electrospray ionization mass spectrometry (ESI-MS) as analytical probes, heptakis(2,6-di-*O*-methyl)-β-cyclodextrin (DIMEB, **3**, Scheme 1) was chosen because of its dimensions and enhanced water solubility.[14] In fact, we soon realized that, among the usual unsubstituted cyclodextrins (α-, β- and γ-CD), only β-CD was a good host capable of forming inclusion complexes, but its water solubility was not as high as that of the EC-DIMEB complex.

The present investigation addresses the definition of structural parameters (such as stoichiometry, binding constants and 3D structural details) of the title inclusion complex EC-DIMEB, as obtained through 1D NMR titration experiments, 2D NMR spectra, ESI-MS measurements and Molecular Mechanics (MM) calculations. Furthermore, a comparative investigation of the hydrolytic instability of EC was carried out on sonicated aqueous samples of EC alone and of the EC-DIMEB complex and a general discussion of this topic is also reported.

Results and Discussion

^{1}H NMR Spectra

Scheme 1 shows the structures with the numbering used for spectral assignments both for EC and DIMEB. Assignments of their relevant protons before complexation were done by ^{1}H NMR analysis (gCOSY, and 1D TOCSY) in deuterated ammonium acetate (CH_3COOND_4 0.8 mM) buffered D_2O using concentrations near to the limit concentration of the complex (see Exp. Sect.).

The complex EC-DIMEB was obtained as a white powder and its stoichiometry was guessed at first by a simple NMR experiment on the dried solid (1.5 mg) dissolved in CD_3OD. The corresponding ^{1}H NMR spectrum, acquired with a relaxation delay long enough to allow complete recovery of longitudinal magnetization, showed that the ratio between the signal area of H-1′ of DIMEB and of H-15 of EC is 7.0 ± 0.1, in excellent agreement with the 1:1 EC-DIMEB relative molar ratio. In this solvent, as expected, no significant chemical shift displacement of the host or guest molecule was found, strongly indicating that the eventual host−guest interaction was completely destroyed by a stronger interaction of the guest with methanol.

On the other hand, when the same amount of the above-cited dried solid was dissolved in D_2O, the ^{1}H NMR spectrum showed a significant shielding effect of the internal protons H-3′ and H-5′ of DIMEB, confirming "incorporation" of the guest and leading to unequivocal proof of non-covalent interactions between the two molecular species. An even stronger downfield effect (complexation-induced chemical shifts, CICS) was also detected for almost

all the EC protons, as reported in the last column of Table 1.

Table 1. Chemical-shifts δ_H (ppm) of free EC and EC-DIMEB complex (0.8 mM) as obtained by ^{1}H NMR (600 MHz, D_2O containing equimolar CH_3COOND_4, 25 °C)

H-type	δ_H (EC)	δ_H (EC-DIMEB)
1	5.61	5.83
2	1.80	1.90
3	2.51	2.75
4α	1.81	1.96
4β	2.18	2.38
5α	1.35	1.46
5β	1.89	2.07
6	1.95	1.91
8	1.96	2.05
9	1.92	2.01
10	5.02	4.98
Me-12	1.59	1.66
Me-13	1.51	1.56
14	6.00	6.14
15	5.81	5.97
MeCO	1.89	2.06

^{1}H NMR detection was also used to investigate the rapid reversible complexation[15] through suitable titration experiments. When host (DIMEB) and guest (EC) interact in solution forming a EC-DIMEB complex, the stability constant K can be easily expressed as a function of their analytical concentrations and of the equilibrium concentration of the complex. In principle, NMR titration experiments can be carried out either by addition of increasing known amounts of the guest to an initial analytical concentration of the host, or vice versa. The low water solubility of free EC does not allow the use of DIMEB as titrating reagent; EC molecules are, in fact, strongly entangled in macromolecular aggregates in water and free EC concentration is rather lower than its analytical concentration. In fact, the area of EC signals in the ^{1}H NMR spectrum of EC in D_2O (even after sonication) was about an order of magnitude lower than expected. Hence we were forced to carry out the titration by adding increasing amounts of EC to a suitable total concentration of DIMEB. The latter was finally chosen to be 1.43 mM in order to avoid solubility limitations due to precipitation of the 1:1 EC-DIMEB complex in the last part of titration curve. Moreover, we prepared each NMR sample separately in order to avoid (or at least to minimize) systematic errors due to the lability of EC towards hydrolysis.

If the solvent effect is ignored and the behavior of all the species in dilute solution is assumed ideal, the stability constant K can be calculated according to the Benesi−Hildebrand equation[16] or by other graphical methods. All common linearization methods,[17] however, failed in our case, whereas non-linear analysis, using the HYP NMR program [18] which allows data-regression for multiple equilibria, suggested the existence of the complex either in 1:1 or in 1:2 (EC-DIMEB) stoichiometry, affording for the corresponding binding constants the estimated values $K_{11} = 1050 \pm 50$ and $K_{12} = 830 \pm 80$.

The stoichiometry of the complex was confirmed by a Job plot ,[19] following Δδ values for H-3′ and H-5′ of DIMEB. Keeping the total concentration constant, but varying the molar ratio [EC]/[DIMEB], the dependence of Δδ values from [EC]/([EC] + [DIMEB]) ratio was observed to be parabolic with the apex at 0.46, corresponding to a mixed 1:1 and 1:2 stoichiometry (Figure 1). Moreover, guessing $r_{max.} = ar_{1:1} + br_{2:1}$, near equimolarity would require 75% of 1:1 EC-DIMEB complex and 25% of 1:2 EC-$(DIMEB)_2$ complex. Assuming the values of binding constants as established by NMR titration experiments, speciation of EC in 1:1 and 1:2 complexes could be easily evaluated for every value of the EC/DIMEB ratio. The results of this calculation (Figure 2) showed that the contribution of 1:2 complex played a significant role only for the lowest EC/DIMEB ratio (large molar excess of DIMEB), whereas in the highest region (large molar excess of EC) 1:1 stoichiometry was expected to be strongly favored. Furthermore, at the equimolar EC/DIMEB ratio, Figure 2 showed that the total amount of the 1:1 complex in solution is about three times that of the 1:2 complex, in good agreement with the Job plot outcome.

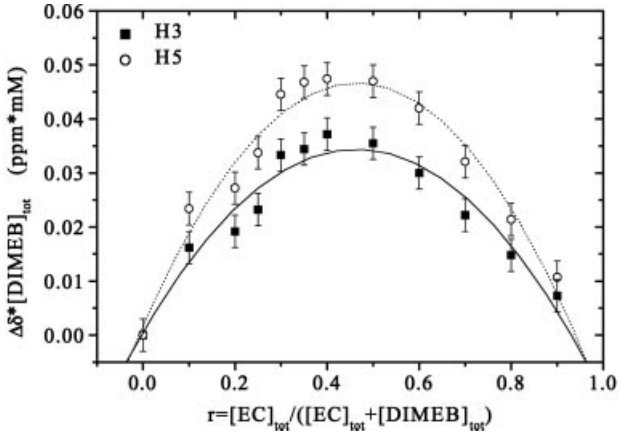

Figure 1. Job plot for EC-DIMEB inclusion complex as obtained from continuous variation method titration

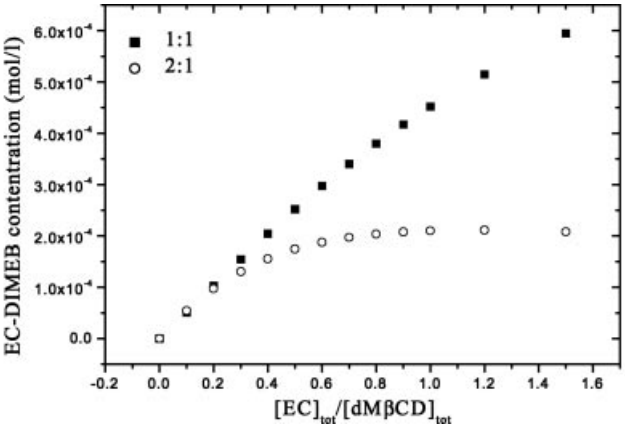

Figure 2. The dependence of the calculated distribution of 1:1 and 1:2 complexes from EC/DIMEB concentration ratio, as obtained with HYP NMR program

Two-dimensional ROESY studies were finally carried out in order to establish the relative disposition of EC and DIMEB in the complex. Figure 3 shows the relevant ROESY traces obtained a few hours after dissolution of 2 mg of the solid EC-DIMEB, having 1:1 stoichiometry, in deuterated ammonium acetate buffered solution (see Exp. Sect.).

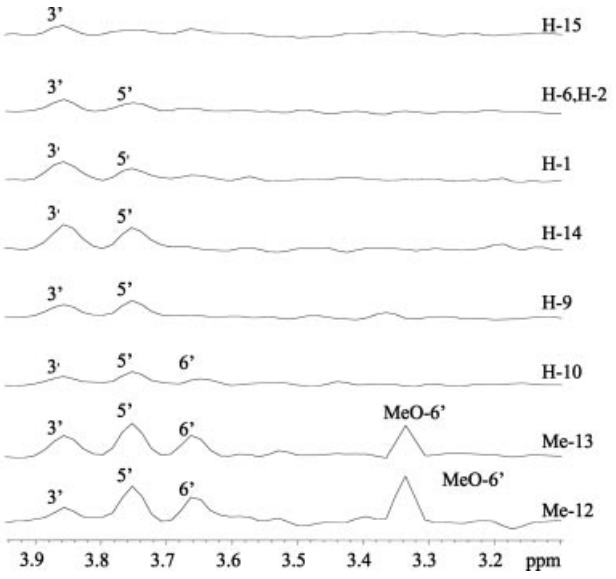

Figure 3. Traces of 2D ROESY map for 1:1 EC-DIMEB complex

The methyl groups linked to double bonds of the lateral chain Me-12 at δ = 1.66 ppm and Me-13 at δ = 1.56 ppm (*cis* and *trans* with respect to the vinyl proton H-10, respectively) produced dipolar interactions with i) the internal protons H-5′ of the hydrophobic cavity, sited towards the smaller rim of DIMEB, ii) the external methylenic diastereotopic protons H-6′ and iii) the methoxy groups at C-6′ lying outside the smaller rim (Figure 4). Me-12 and Me-13 also generate significant NOE enhancements on internal proton H-3′ lying on the large diameter cavity. On the other hand, vinyl proton H-10 showed intense NOE effects with both internal H-5′ and H-3′ (stronger with the first) and a weak one with 2H-6′, while other protons on the side chain, such as 2H-9, displayed interaction only with internal H-3′ and H-5′ (Figure 3).

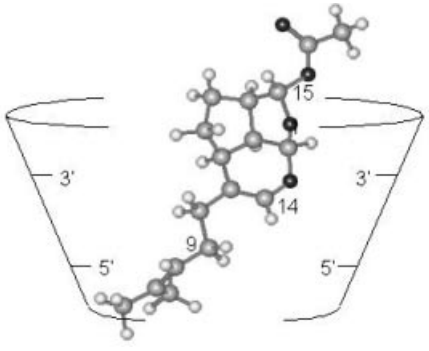

Figure 4. A schematic picture of the 3D-structure for 1:1 EC-DIMEB complex

The dihydropyranic ring protons (H-14, H-1, H-2 and H-6) also induced NOE effects, stronger on H-3′ than on H-5′, the former being near the larger rim of DIMEB. A negligible NOE effect of H-15 on H-3′ was observed (Figure 3) and no dipolar interactions between DIMEB protons and EC cyclopentane ring protons H-4, H-3 and H-5 were detected. All of this evidence confirmed the inclusion phenomenon and was weighted towards a preferential insertion of the guest from the side-chain direction. A reasonable description is that EC enters into the wider rim of the DIMEB cavity (with isopropylidene methyl groups acting like advance guards) and deeply penetrates into it in such a way that the prenyl chain remains exposed to the narrower rim, whereas the acetyl group and the cyclopentane ring protons H-4 and H-5 lie outside the larger rim (Figure 4).

As is well known,[27] and confirmed in the present case, in the formation of cyclodextrin inclusion complexes not only does the molecular motion of the guest compound undergo a significant slowing down but also an independent motion of the substrate with respect to the cavity occurs. Hence the two components of the complex (host/guest) are characterized by different reorientational correlation times. As a consequence, quantitative correlation of intermolecular NOE data to intermolecular distances is quite hazardous, because we have no value of the reorientational correlation time to be used in the calculation of distances from the observed NOE. A further problem is that NOE effects always reflect an ''average'' situation, which is, in our case, even more difficult to analyze quantitatively taking into account the possibility of the coexistence of 1:1 and 1:2 complexes.

Even if we have no clear-cut structural information on the 1:2 complex inferred from titration experiments and ESI measurements (as discussed in the next paragraph), we can guess that here the long axis of euplotin C is normal to the plane of two, head-to-head aligned, DIMEB molecules. With such a structure, the NOE effects reported in Figure 3 might also be consistent with a contribution of 1:2 stoichiometry to the overall equilibrium complexation.

ESI-MS Analysis

Electrospray ionization mass spectrometry (ESI-MS) is a new and emerging technique which has proved very useful in the study of biomolecular noncovalent interactions.[20−24] The results provided by ESI-MS are complementary to those provided by circular dichroism, fluorescence, IR and UV spectroscopic methods and 1D NMR measurements. Since ESI-MS provides an accurate measure of the molecular mass of the complex being studied, the primary information obtained is the stoichiometry of the complex. Unfortunately, typical solvent conditions used in ESI-MS to achieve maximum sensitivity are not always optimal for maintaining the molecular complex itself intact. As a result, ESI may give a more accurate representation of solution equilibria when complexation is dominated by electrostatic forces and is expected to be unreliable when solvophobic interactions are dominant.

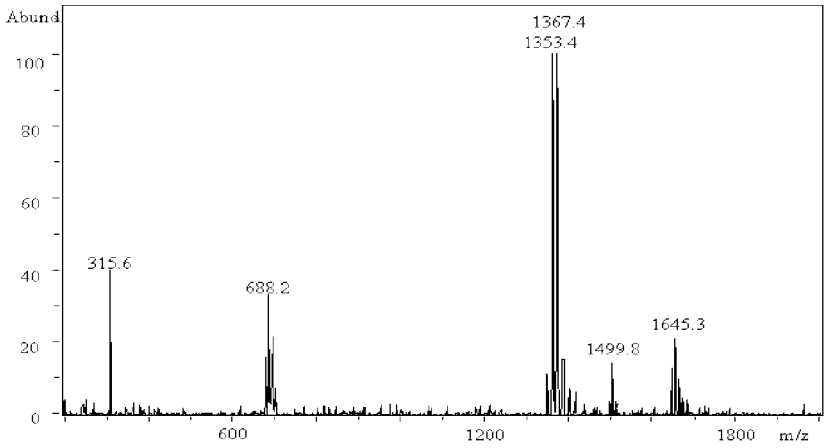

Figure 5. Positive ion mode ESI-MS spectrum of EC-DIMEB (white powder) in water

Since a direct comparison of kind and strength of the relevant interactions in the gas phase was beyond the scope of our work, we subjected our EC-DIMEB complex to ESI-MS analysis with the aim of investigating only the stoichiometry and gas-phase behavior. Thus, an aqueous solution (0.6 mM) containing equimolar amount of EC and DIMEB was directly infused at a flow rate of 2 μL/min into the ESI source in positive-ion mode. Detection and all instrumental parameters were optimized in such a way that the pseudo-molecular ion of the 1:1 complex $[EC\text{-}DIMEB + Na]^+$ at $m/z = 1645$ had the highest signal/noise ratio. Among many factors, the temperature and the flow of the gas nebulizer have been demonstrated to be quite critical, but the skimmer voltage and the trap drive level have also been extensively investigated to find the best compromise (see Exp. Sect.). With reference to the general discussion reported above, we soon realized that the experimental response factors of all the species participating in the complexation equilibrium were widely different and reliable calibration curves for EC and DIMEB could not be obtained under the experimental conditions required for detection of the complex. Furthermore, even assuming a similar ionization efficiency for free and complexed host−guest molecules, the expected wide difference in the volatility of EC and DIMEB under the instrumental conditions used (pressure drop from source to analyzer), hindered any reliable link between analytical (in source) and gas-phase (in the ion trap) equilibrium concentrations.

As shown in Figure 5, we were able to detect the cluster signals for i) free EC as the parent ion $[EC + Na]^+$ at $m/z = 315$, ii) free DIMEB as the parent ion $[DIMEB + Na]^+$ at $m/z = 1353$ (ion at $m/z = 1367$ in the same cluster is also present, as expected, owing to the presence of trimethyl analogues in commercially available DIMEB mixture) and double-charged ions $[DIMEB + 2Na]^{2+}$ at $m/z = 688$, iii) 1:1 complex as the parent ion $[EC\text{-}DIMEB + Na]^+$ at $m/z = 1645$, which roughly reproduces the statistical distribution of methyl substituents in the commercially available DIMEB.

Tandem MS/MS experiments carried out in the ion trap through isolation of the relevant cluster of the 1:1 complex at $m/z = 1645$, and CID fragmentation analysis, afford the daughter ion $[DIMEB + Na]^+$ at $m/z = 1353$ by neutral loss of EC, confirming that non-covalent interactions involved in the gas-phase complex formation were rather weak. Significantly, the ESI mass spectrum of the infused EC-DIMEB solution also contained a low, but detectable, peak centered at $m/z = 1499$, arising from $[EC + 2DIMEB + 2Na]^{2+}$, suggesting the presence in the gas phase of the 1:2 complex. This outcome was in fair agreement with the NMR titration data previously discussed, bearing in mind that 1:2 stoichiometry could play a significant role only at very low values of the [EC]/[DIMEB] ratio (Figure 2).

Confidence in the reliability of our ESI-MS results derives from other control experiments performed on aqueous solutions obtained by adding EC to α- and γ-CDs. Under such conditions, no MS signal attributable to EC-CD inclusion complexes was eventually detected, in good agreement with NMR spectra, which did not reveal any evidence of complexation of EC with α- and γ-CDs. Such agreement between NMR (solution) and ESI-MS (gas-phase) data for EC-DIMEB complexes was, however, not observed in the ESI-MS analysis of pure DIMEB samples. In fact, whereas ESI-MS measurements showed the presence in the gas phase of signals for mono- and double-charged pseudo-molecular ions attributable to a dimeric form of DIMEB (self-association), ^1H NMR experiments on samples containing increasing (and high) amounts of DIMEB did not reveal any concentration dependence for the chemical shifts of DIMEB's protons. Because of the ionization mechanism, in-source electrostatic aggregations of DIMEB could possibly generate supramolecular clusters in the gas phase. Actually, the existence of CD dimers in vacuo, recently suggested for β-cyclodextrin from Molecular Dynamics calculations,[25] seems to find here an experimental verification, at least for DIMEB.

Solubility Investigations

Euplotin C can be considered an amphiphilic molecule since it contains a "water-like" polarized part of the tricyclic ring system defined by a peculiar 1−3−5−7 sequence of electron-withdrawing oxygen atoms whereas the remain-

ing part represents a hydrophobic moiety. It is therefore not surprising that EC can give rise to micellar aggregates in water, at least above its critical concentration (CMC). Thus, while below CMC all dissolved euplotin C is monomeric, above CMC the concentration of monomers remains low and approximately constant. Although we did not measure either the CMC value of euplotin C in aqueous solution or the real size of its aggregates, clear-cut evidence of a micellar phase came from ^{1}H NMR spectra taken on aqueous samples containing different euplotin C concentrations. Since the molar absorptivity of EC at its maximum absorption ($\lambda_{max.}$ = 215 nm) is not changed by complexation, a simple UV analysis showed that DIMEB is able to increase the solubility of EC in water by three orders of magnitude, until the solubility limit (1.40 mM) of the 1:1 EC: DIMEB complex itself is reached. In artificial seawater the complex solubility is, however, significantly lower (0.85 mM), as expected from the salting-out effect.

Molecular Mechanics Calculations

The distance of EC from the mean plane formed by the linker oxygens in DIMEB is critical in the search for the global minimum. As EC approaches DIMEB, the energy of the system begins to decrease, but as EC moves deeper inside and away from the inclusion complex cavity (Figure 6), the overall energy of the system begins to increase, reaching the initial value given by summation of the EC and DIMEB isolated strain energies. Since DIMEB does not have true cylindrical symmetry, the conformational space around EC must be widely sampled in order to find the real minimum of the inclusion complex since a high number of rotamers are expected to exist.

The calculated strain energies also depend on the orientations of the methoxy and hydroxy groups in DIMEB and on the torsional angles along the chain in EC. The total expected number of all the possible combinations becomes so high that it overwhelms any hope of explicit consideration. In fact, in the present work only a single combination of the group's orientations has been considered and the same initial conformation of DIMEB was used during each minimization step. The binding energy obtained from the difference between the two limiting situations − the first having the side chain and the second having the ring system of EC inserted from the wider rim of DIMEB − are 18.8 and 15.7 kcal/mol respectively, suggesting a significant preference (2.9 kcal/mol) for the former. Figure 7 presents the minimized structure of the 1:1 complex, which nicely fits the NMR spectroscopic data, showing that the EC guest is inserted well into the DIMEB cavity.

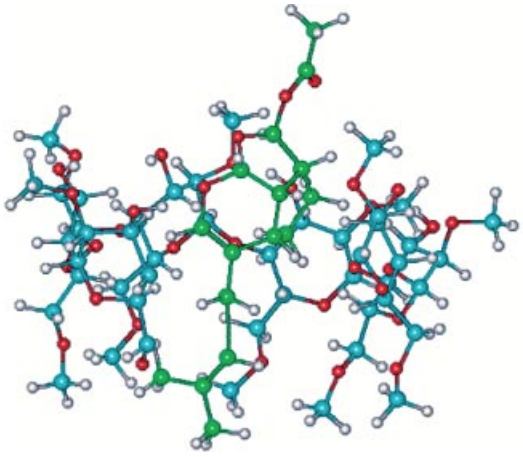

Figure 7. MM3 computed minimum structures of EC-DIMEB 1:1 inclusion complex. Carbon atoms of EC are colored green to better distinguish the guest from the host skeleton. The front part of DIMEB structure has been deleted for the sake of clarity

For the computational approach, we preferred to use molecular mechanics and not semi-empirical quantum mechanical methods since the former require less computational resources than the latter and, more important, semi-empirical quantum mechanical calculations have not proven adequate for cyclodextrin structures.[12]

Euplotin C Hydrolysis

As already described,[1c] EC undergoes rapid hydrolytic degradation in mild basic conditions. On the other hand, NMR measurements on the EC-DIMEB complex suggested that these phenomena were somehow also operating in a neutral aqueous medium. In order to understand

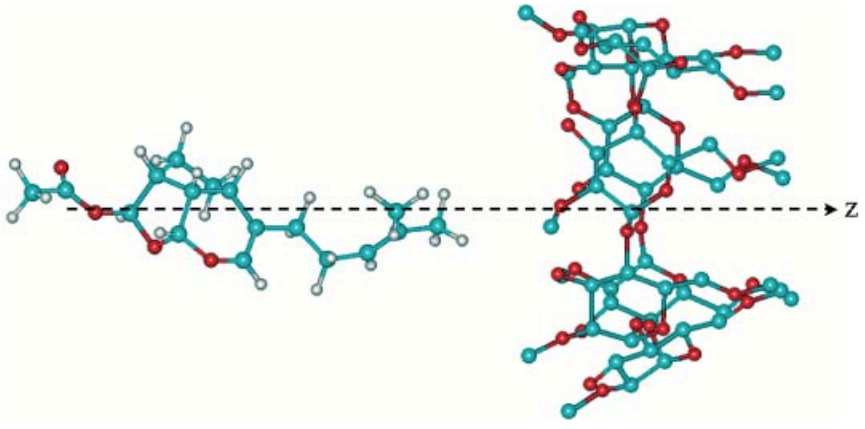

Figure 6. MM3 computed minimum structures of EC (left) and of DIMEB (left). Hydrogen atoms are not drawn in DIMEB for the sake of clarity. Dotted arrow (*z*-axis) represents the direction along which EC approaches the wider edge of the host torus

whether EC degradation could be catalyzed (or inhibited) to some extent by its inclusion in the cyclodextrin cavity, we carried out kinetic investigations on both the EC-DIMEB complex and on free EC aqueous solutions prepared at the same initial EC concentration (0.15 mM), using the LC-Photodiode array (PDA)-MS/MS as probe technique.

Reversed-phase HPLC-UV-MS analysis of water solutions (see Exp. Sect.) of the EC-DIMEB complex confirmed the slow degradation of EC (Figure 8) already observed at higher concentrations during NMR measurements, and allowed identification of the end products (Scheme 2).

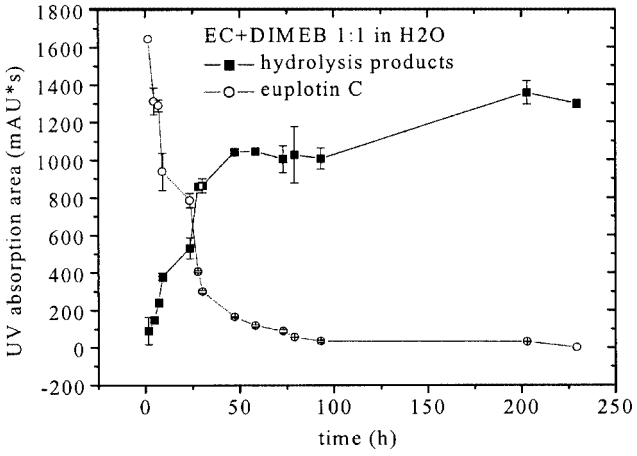

Figure 8. Time dependence of UV-detected EC (dotted line) and of its hydrolysis products **2a**−**4a** (solid line) during the degradation of EC-DIMEB complex in water

Formation and fast disappearance of the chromatographic peak with ESI-MS signals at $m/z = 273$ and attributable to the parent ion $[M + Na]^+$ of the hemiacetal **2a**, were thus seen to be followed by the appearance, at shorter retention times, of a series of partially resolved peaks at $m/z = 291$, attributable to the parent ions $[M + Na]^+$ of diastereoisomeric mixture **3a** which was observed to grow continuously during the reaction course until the complete disappearance of EC (detectable as the longest retention time peak having ESI-MS signals at $m/z = 315$). In further support of our mechanistic interpretation, when the EC-DIMEB complex was dissolved in deuterated water, epimeric mixture **3b**, whose retention time was the same as that of **3a**, but whose parent ion $[M + Na]^+$ was detected at 3 Da higher ($m/z = 294$), was detected. Although MS analysis could not discriminate among all the possible isomeric forms of **3a** or **3b** in protic solvents, we are confident in the proposed tricyclic ring structure since, during NMR measurements on the EC-DIMEB complex carried out in similar conditions, a large upfield shift of H-7 and H-15 resonances was observed. At room temperature the half-life of complexed EC was roughly estimated to be 16 h from the exponential decay of the EC signal as detected by HPLC-PDA analysis (Figure 8). While the concentration of mixture **3a** was still increasing, more polar compounds **4a** appeared as a broad peak in the HPLC profile. Our proposed structures **4a** (and the corresponding **4b** when using D_2O) for these compounds derived from NMR spectral analysis of the EC-DIMEB complex taken two days after its preparation. An upfield shift of the isopropylidene Me protons and the disappearance of the olefinic proton on the side-chain were indeed easily detected. Figure 8 also shows the total integrated UV area versus the time of hydrolysis for all the identified products **2a**−**4a**.

In conclusion, therefore, three chemical processes seem to operate during EC-DIMEB degradation: i) initial acetyl cleavage affording **2a**, ii) electrophilic water addition to the activated vinyl ether double bond affording **3a** and iii) electrophilic water addition catalyzed by acetic acid present in the reaction medium to the trisubstituted double bond of the side chain leading to the end products **4a**. While the first two reactions occur with similar rate constants, the latter is significantly slower and becomes significant only after complete disappearance of EC. Open free aldehyde isomers are expected to be labile intermediates playing an equilibration role among detectable hemiacetal intermediates.

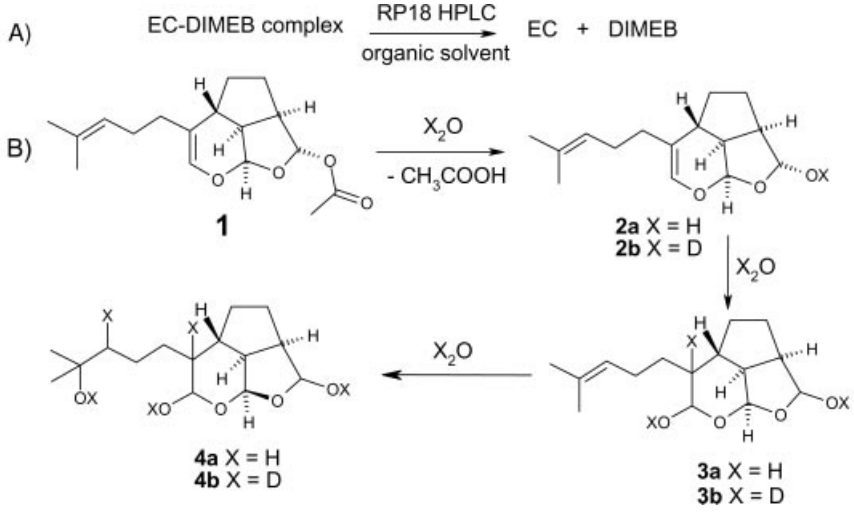

Scheme 2. Chemical transformations of **1** in water (X = H) and in deuterated water (X = D) solution

In order to establish the existence of an inhibitory (or catalytic) effect of DIMEB on the kinetics of EC degradation in water, we turned our attention to aqueous solutions of EC alone. Kinetics measurements on these solutions showed similar general features to those previously observed for the EC-DIMEB complex (Figure 9). Since EC is sparingly soluble in water, even at the low concentration used in our experiment, it is mainly present in this solution as molecular aggregates that can be only partially resized by sonication. This explain the different detected value of the EC area at the beginning of our measurements (about 500 mAU×s in Figure 9 compared with 1600 mAU×s in Figure 8).

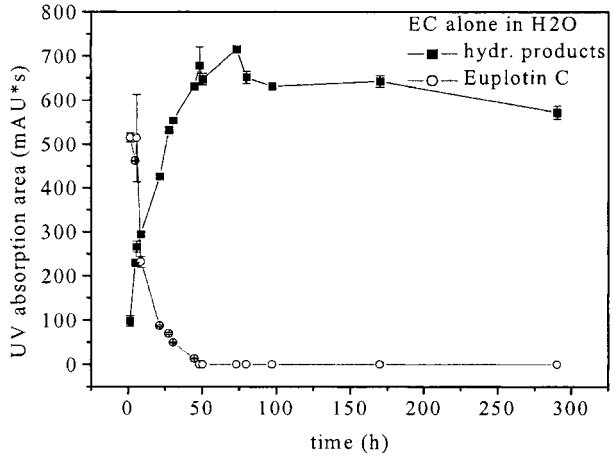

Figure 9. Time dependence of UV-detected EC (dotted line) and of its hydrolysis products **2a**−**4a** (solid line) during the degradation of EC in water

Nevertheless EC hydrolysis provided the same products **2a**−**4a** as observed for EC-DIMEB complex degradation through faster processes with an estimated half-life of 7 h at room temperature.

Micellar catalysis[26] seems to play a key role here. In general terms, increasing the reactant (EC) concentration in the micellar phase could lead to a considerable acceleration of the hydrolysis reaction. Such distribution phase equilibria play an important role in the overall hydrolytic process and hinder the interpretation of kinetic data. Nevertheless, a comprehensive kinetics study on these systems (changing the boundary conditions and evaluating the relevant rate parameters) is currently under investigation in our laboratory.

Conclusion

The inclusion complex between euplotin C and β-cyclodextrin (or its derivatives) was fully characterized using 1D and 2D NMR techniques and LC-ESI tandem MS measurements. Stoichiometry, binding constants and the three-dimensional structure of the 1:1 inclusion complex have been determined but our data also suggests that, in solution, EC/DIMEB (1:2) stoichiometry cannot be ruled out even if its contribution is negligible at low DIMEB/EC ratios. Furthermore, the present study highlights the increased solubility and the increased chemical stabilization from hydrolysis of EC-DIMEB complexes compared with free EC, suggesting that these complexes can be used in the next biological tests as reliable EC sources, avoiding the use of organic solvents (such as DMSO[1−3]) as the carrier agent for such hydrophobic compounds in the biotests.

Experimental Section

Materials: Heptakis(2,6-di-*O*-methyl)-β-cyclodextrin (DIMEB) from Sigma−Aldrich was used without further purification. Merck deuterium oxide (D_2O, 99.9%) and Merck deuterated methanol (CD_3OD, 99.95%) were used as NMR solvents. All the HPLC solvents were purchased from Riedel de Haën. For NMR experiments, DIMEB was subject to preliminary deuterium exchange by repeated evaporations of its D_2O solutions. Deuterated ammonium acetate ($CH_3COO^-ND_4^+$), was obtained by repeated D_2O exchange from ammonium acetate (Merck) and used for preparing buffer solutions. Flash chromatography (FC): Merck Kieselgel Si-60 15−25 μm. HPLC: Reversed-phase HPLC: Agilent Zorbax Eclipse XDB-C18 150 × 4.6 mm (3.5μm) or Merck LiChrosphere RP-18 250 × 10 mm (7 μm). TLC: Merck Kieselgel 60.

E. crassus cells (strain SSt22) harvested from mass cultures were closely packed forming pellets by centrifugation. The pellets were suspended in absolute ethanol, but the culture fluid was discarded because it did not contain any sesquiterpenes. Since the attempt to improve sesquiterpene extraction by breaking cell walls using sonication was unsuccessful, cell suspensions were filtered, the alcoholic filtrate evaporated and the residue partitioned between *n*-hexane/ethyl acetate (8:2) and H_2O. The organic extract was worked up to obtain pure euplotins and preuplotin by initial flash chromatography on Si60 (20−40 μm) collecting 17 fractions (40 mL) and using *n*-hexane/ethyl acetate gradient elution. Fractions of interest (tested on TLC Si60) were finally purified with an HPLC Merck−Hitachi L6200 pump and an L3000 Photo Diode Array (PDA) detector system using a Merck LiChrosphere Si60, 250 × 10, 5 μm column. The mobile phase was *n*-hexane/ethyl acetate 97/3 and the detector wavelength λ = 215 nm. From 15.0 mL of cell pellet of *E. crassus* strain SSt22 we obtained 17 mg of pure EC (**1**).

The EC-DIMEB complex was obtained by adding 5 mL of 22.6 mM DIMEB aq. solution to an equimolar amount of dry EC, prepared by evaporation from its mother solution (stored in *n*-hexane at −20 °C before use). The incipient emulsion was then stirred for 30 min at 40 °C and sonicated for 30 min. Complex formation was indicated by the precipitation of a white solid which was isolated by filtration, washed with distilled water and dried under vacuum by variable pressure cycles in a vacuum chamber connected to a rotary pump.

Methods: NMR spectra (gCOSY, 1D TOCSY, 2D ROESY) were recorded in D_2O buffered solution (CH_3COOND_4 0.8 mM) with a Varian Inova 600 spectrometer operating at 599.686 MHz for ^1H using a 5-mm broadband inverse probe with *z*-axis gradient. ^1H NMR spectra for titrations and the continuous variation method were recorded in D_2O/CH_3COOND_4 (0.8 mM) with a Varian XL-300 spectrometer operating at 299.909 MHz for ^1H. Chemical shifts are referenced to TMS using the residual water signal at δ = 4.72 ppm. All NMR spectra were recorded at 25.4 ± 0.1 °C.

Proton gCOSY 2D spectra were recorded in the absolute value mode acquiring eight scans with a 2-s relaxation delay between acquisitions for each of 128 FIDs. The ^{1}H 90° pulse width was 8.3 μs. Proton 1D TOCSY spectra were recorded using selective pulses generated by means of the Varian Pandora Software. Selective 1D TOCSY spectra were acquired with 256−512 scans in 32 K data points with a relaxation delay of 2 s and a mixing time of 80 ms. 2D ROESY spectra were recorded in phase-sensitive mode, employing a mixing time of 0.6 s. The spectral width used was the minimum required in both dimensions. Pulse delay was maintained at 2 s; 256 hypercomplex increments of eight scans and 2 k data points each were collected. The data matrix was zero-filled to 2 k × 1 k and a Gaussian function was applied for processing in both dimensions.

NMR titration measurements for the Job plot were taken on 12 samples all containing 1 μmol of total EC + DIMEB; this was obtained by appropriate additions into the corresponding 5-mm NMR tubes of increasing amounts of EC (evaporated before use from the 3.4 mM mother *n*-hexane solution) and decreasing amounts of DIMEB (taken from a 17.1 mM D_2O mother solution); the same amount (1.0 μmol) of the buffer solution, 0.8 mM CH_3COOND_4, was finally added and the final volume in the NMR tubes was adjusted to 600 μL by different D_2O volumetric aliquots. Every sample was sonicated for at least 30 min before spectrum acquisition.

NMR titration was made on 13 samples containing 0.86 μmol of DIMEB and increasing amounts of EC (0−1.28 μmol) in 600 μL of D_2O/CH_3COOND_4 (0.8 mM) prepared as above. All samples were sonicated for at least 30 min before acquiring spectra.

NMR spectroscopic data were then analyzed with non-linear analysis program HYP NMR spectroscopy.[18]

LC-MS analysis was performed on a Hewlett−Packard Series 1100 liquid chromatograph coupled to a Bruker Esquire-LC™ ion trap mass spectrometer equipped with an atmospheric pressure ESI interface. A Rheodyne 7725 (Cotati, CA, U.S.A.) injection valve equipped with a 20-μL internal loop was used for the injections. The PDA (Photo Diode-Array) detector (HP Series 1100) was set at a wavelength of 215 nm, and a 7:3 split of the column effluent was used to achieve a flow rate of 300 μL/min into the ESI source.

Samples (0.6 mM aqueous solution containing equimolar amounts of EC and DIMEB) were directly infused at a flow rate of 2 μL/min into the ESI source set in positive-ion mode detection with a voltage of 4000 V, scan range 100−2000 *m*/*z* and nebulizer gas pressure at 20 psi; high-purity nitrogen was used also as a dry gas, at a constant flow rate of 4 L/min and heated to 200 °C.

Kinetics measurements were performed by HPLC/PDA/ESI-MS under the following conditions: Agilent Zorbax Eclipse XDB-C18 4.6 × 150 mm, 3.5 μm, column CH_3CN/H_2O 7:3, flow 0.5 or 0.9 mL/min, split UV/MS 7:3, UV range 200−350 nm, detection at 215 nm. MS conditions: source temp. 300 °C, nebulizing gas N_2 4 L/min, positive ion mode, ISV 4 kV, OV 52V, scan range 100−2000 *m*/*z*.

Twenty 0.15 mM aq. solutions of EC, without and with DIMEB, were prepared (all at the same time and sonicated before every analysis) and then the same aliquot (20 μL, 0.8 μg of total EC on the column) at appropriate time intervals was injected in RP18 HPLC to obtain both UV and MS profiles. The EC molar concentration in all performed analyses was established by the appropriate calibration curve (UV detected peak area) vs [EC], whereas the ESI-MS profile was used as a qualitative probe for reaction monitoring.

Molecular Mechanics calculations were done using the PCMODEL 7.0 program (Serena Software) using the MM3(96) force field. Preliminary minimized structures for EC and DIMEB were obtained on their input structures; they were then optimized by full conformational search around the rotatable bonds using the GMMX program. The minimum conformation of EC and DIMEB was finally minimized by the MM3 force field and the corresponding structures were used in the subsequent calculations. Orientation of the guest entering the larger side of the cavity, depth of penetration and rotational orientation of the guest with respect to the plane of the host's glucose residues were then evaluated by MM3 calculations. For the first variable, the guest was initially placed at a distance of 17 Å from the mean plane of the linkage oxygen atoms. It was centered on a vector normal to that mean plane, and was moved in decreasing increments with the side chain towards the center of the cavity. The same procedure was then followed with the tricyclic system entering the cavity. Once the guest began to penetrate the host, increments were reduced, allowing the guest to go more slowly through the cavity. Then increments were increased and the guest moved away from the host to 17 Å beyond the plane of the linkage oxygens. Calculations were also performed without distance constraints: putting EC and DIMEB at a suitable initial geometrical disposition (with the EC side chain perpendicular to the mean plane of the acetal oxygen atoms), the system was allowed to reach the final minimum energy.

Acknowledgments

We thank Adriano Sterni for skilled assistance in ESI-MS measurements and Francesco Frontini for helping us in growing *E. crassus* cell cultures. Work was financially supported by PRIN2001 MURST project and by local funds of the involved Departments.

[1] [1a] F. Dini, G. Guella, P. Giubbilini, I. Mancini, F. Pietra, *Naturwissenschaften* **1993**, *80*, 84−86. [1b] G. Guella, F. Dini, T. Tomei, F. Pietra, *J. Chem. Soc., Perkin Trans. 1* **1994**, 161−166. [1c] G. Guella, F. Dini, T. Tomei, F. Pietra, *Helv. Chim. Acta* **1996**, *79*, 710−717.
[2] F. Trielli, G. Guella, G. Di Giuseppe, B. Burlando, A. V. Corrado, T. Kruppel, A. Viarengo, F. Dini, manuscript submitted.
[3] D. Savoia, G. Guella, E. Callone, F. Dini, work in progress.
[4] T. Nakatsu, B. N. Ravi, D. J. Faulkner, *J. Org. Chem.* **1981**, *46*, 2435−2438.
[5] R. A. Aungst Jr., R. L. Funk, *J. Am. Chem. Soc.* **2001**, *123*, 9455−9456.
[6] K. A. Connors, *Chem. Rev.* **1997**, *97*, 1325−1357.
[7] K. Miyake, F. Hirayama, K. Ukeama, *J. Pharm. Sci.* **1999**, *88*, 39−45.
[8] A. M. C. Myles, D. J. Barlow, G. France, M. J. Lawrence, *Bioch. Bioph. Acta* **1994**, *1199*, 27−36.
[9] N. Nesnas, J. Lou, R. Breslow, *Bioorg. Med. Chem. Lett.* **2000**, *10*, 1931−1933.
[10] I. Tabushi, *Acc. Chem. Res.* **1982**, *15*, 66−72.
[11] S. Li, W. C. Purdy, *Chem. Rev.* **1992**, *92*, 1457−1470.
[12] K. Lipkowitz, *Chem. Rev.* **1998**, *98*, 1829−1873.
[13] W. Saenger, *Angew. Chem.* **1980**, *92*, 343−361; *Angew. Chem. Int. Ed. Engl.* **1980**, *19*, 344−362.
[14] M. Taghvaei, G. H. Stewart, *Anal. Chem.* **1991**, *63*, 1902−1904.
[15] T. Wang, J. S. Bradshaw, R. M. Izatt, *J. Heterocycl. Chem.* **1994**, *31*, 1097−1114.

[16] H. A. Benesi, J. H. Hildebrand, *J. Am. Chem. Soc.* **1949**, *71*, 2703−2707.
[17] L. Fielding, *Tetrahedron* **2000**, *56*, 6151−6170.
[18] C. Frassineti, S. Ghelli, P. Gans, A. Sabatini, M. S. Moruzzi, A. Vacca, *Anal. Biochem.* **1995**, *231*, 374−382.
[19] [19a] P. Job, *Ann. Chim. Appl.* **1928**, *9*, 113−134. [19b] F. Djeaini, S. Z. Lin, B. Perly, D. Wouessidjewe, *J. Pharm. Sci.* **1990**, *79*, 643−646.
[20] J. B. Cunniff, P. Kouros, *J. Am. Soc., Mass Spectrom.* **1995**, *6*, 437−443.
[21] M. Shahgholi, C. L. Copper, J. Callahan, *Supramol. Chem.* **1998**, *9*, 263−276.
[22] C. Siethoff, W. Wagner-Redeker, M. Schaefer, M. Lindscheid, *Chimia* **1999**, *53*, 484−491.
[23] J. B. Fenn, M. Mann, C. K. Meng, S. F. Wong, C. M. Whitehouse, *Science* **1989**, *246*, 64−71.
[24] R. B. Cole, *Electrospray Ionization Mass Spectroscopy*, Wiley-Interscience, New York, **1997**.
[25] P. Bonnet, C. Jaime, L. Morin-Allory, *J. Org. Chem.* **2001**, *66*, 689−692.
[26] S. Tascioglu, *Tetrahedron* **1996**, *52*, 11113−11152..
[27] G. Uccello-Barretta, C. Chiavacci, C. Bertucci, P. Salvadori, *Carbohydr. Res.* **1993**, *243*, 1−10.

Received August 5, 2003

